

ANGULAR DISTRIBUTIONS IN THE REACTION ${}^6\text{Li}(p, {}^3\text{He}){}^4\text{He}^\dagger$ G. P. JOHNSTON^{††} and D. G. SARGOOD*School of Physics, University of Melbourne, Victoria, Australia*

Received 25 February 1974

Abstract: Angular distributions in the reaction ${}^6\text{Li}(p, {}^3\text{He}){}^4\text{He}$ have been measured over the energy range 0.5–1.82 MeV. Two particle pick-up theory is used to analyse the results and, with a constant normalisation factor of 0.3, it accounts well for the observations below 1.3 MeV and for the non resonant yield above 1.3 MeV.

E NUCLEAR REACTIONS ${}^6\text{Li}(p, {}^3\text{He})$, $E = 0.5\text{--}1.82$ MeV, measured $\sigma(E, \theta)$.
Deduced reaction mechanism. Enriched target.

1. Introduction

It has been known for many years ^{1,2)} that the angular distributions of the product particles in the reaction ${}^6\text{Li}(p, {}^3\text{He}){}^4\text{He}$ at low bombarding energies are strongly asymmetric about 90° . In an attempt to fit the angular distributions theoretically on the basis of compound nucleus theory, Marion *et al.* ¹⁾ postulated the existence of a $\frac{3}{2}^+$ level at ≈ 6.5 MeV in ${}^7\text{Be}$, and suggested that the reaction proceeded via this level and the broad $\frac{5}{2}^-$ level at 7.19 MeV in ${}^7\text{Be}$. Beaumevielle *et al.* ²⁾ showed that this postulate was not sufficient to account for the data over the whole proton energy range from 130 keV to 3 MeV and found it necessary also to postulate two additional $\frac{3}{2}^-$ levels in ${}^7\text{Be}$, one at 9.5 MeV and the other at 5.9 MeV.

Since none of these postulated states has been observed experimentally it seems appropriate to look for an alternative mechanism for the reaction. Perhaps the simplest alternative is to consider a two particle pick-up process, in which the incident proton picks up a loosely bound proton-neutron pair from the ${}^6\text{Li}$ target, to form a ${}^3\text{He}$ nucleus and leave an α -particle as the residual nucleus. If such a mechanism is important in this reaction it will be most readily observed at bombarding energies well removed from known resonant energies, so that any compound nucleus contribution to the cross section will be small.

The lowest energy resonance in ${}^6\text{Li} + p$ occurs at a proton energy of 1.82 MeV. It was therefore decided to make a detailed series of measurements on the angular distribution over the proton energy range from 0.5 MeV up to 1.82 MeV.

[†] Supported in part by The Australian Institute of Nuclear Science and Engineering, and the Australian Atomic Energy Commission.

^{††} Present address: Kodak (Australasia) Pty. Ltd., Coburg, Victoria.

2. Experimental details

2.1. REACTION KINEMATICS

The reaction ${}^6\text{Li}(p, {}^3\text{He}){}^4\text{He}$ has a positive Q -value of 4.02 MeV, so both ${}^3\text{He}$ and ${}^4\text{He}$ particles left the target with easily detectable energies. By detecting both ${}^3\text{He}$ and ${}^4\text{He}$ particles at each angle of observation, it was possible to limit observation to the backward hemisphere, the forward hemisphere yield of ${}^3\text{He}$ being inferred from the

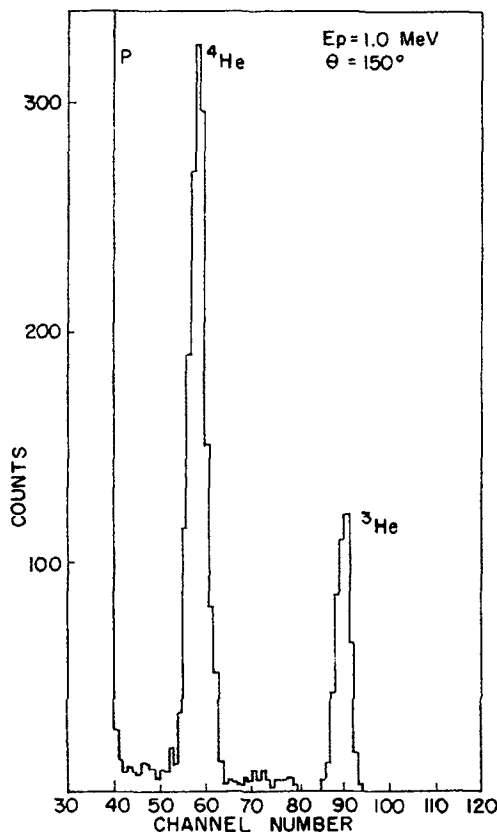


Fig. 1. Typical pulse height spectrum.

${}^4\text{He}$ measurements. This allowed all observations to be made in a region where the flux of elastically scattered protons was sufficiently low that there was no need to exclude them from the detector, thus eliminating the need for magnetic analysis. A typical pulse height spectrum is shown in fig. 1.

2.2. TARGETS

Thin oxidised ${}^6\text{Li}$ targets with $\approx 30 \mu\text{g}/\text{cm}^2$ of lithium, were prepared by evaporating 99.6% ${}^6\text{Li}$ separated isotope onto backings of nickel, $0.1 \mu\text{m}$ in thick-

ness, in vacuum, and then exposing the target to the atmosphere. Some targets were prepared in the scattering chamber itself and were not oxidised, but these proved less durable than the oxidised targets. Only very thin target backings were used to keep the yield of Rutherford scattered protons within the limits which could be tolerated by the detector. To prepare these backings, thin copper foils coated on one side with a $0.1\text{ }\mu\text{m}$ electrolytically deposited nickel layer[†], were placed nickel face down on aluminium frames which carried a thin layer of epoxy resin, and after the epoxy had cured the copper foil was dissolved away, using the techniques described by Bashkin and Goldhaber³).

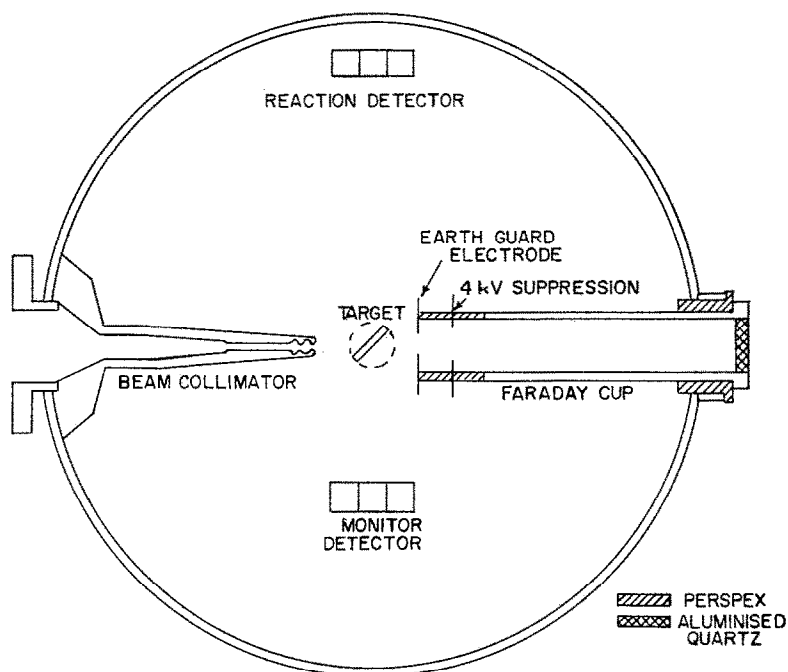


Fig. 2. Experimental layout in the scattering chamber.

2.3. EXPERIMENTAL APPARATUS AND PROCEDURES

Proton beams were obtained from the University of Melbourne 900 keV electrostatic accelerator and from the 3 MeV Van de Graaff accelerator at the Australian Atomic Energy Commission Research Establishment. The protons entered the scattering chamber, shown in fig. 2, and after collimation struck the lithium coated side of the target which was oriented at 45° to the beam direction. The transmitted proton beam entered a Faraday cup which had a 4 kV electron suppression electrode.

[†] Supplied by the Chromium Corporation of America.

The yield of ^3He and ^4He was measured at 10° intervals from 70° to 160° in the laboratory, using an Ortec SBCJ-025-300 surface barrier detector. The beam current integrator, connected to the Faraday cup, and the ^3He yield in a second detector fixed at an angle of 90° to the incident beam, were used as independent monitors for the angular distribution measurements. The consistency observed between these two monitors was good evidence that the targets did not deteriorate under bombardment. To check that there was no systematic drift in the system the observations were made at 20° intervals from 160° to 80° and then at 20° intervals from 70° to 150° , and finally the 160° measurement was repeated. Angular distributions were measured at proton energies of 0.5, 0.6, 0.69, 0.79, 0.89, 0.99, 1.09, 1.19, 1.29, 1.4, 1.5, 1.6, 1.7, and 1.82 MeV. At the higher energies, protons scattered to the more backward angles were of energy comparable to that of the ^4He group, and rendered this group unobservable. Hence the ^3He yield at the corresponding forward angles could not be inferred, and the angular distributions do not cover the full range of angles used at the lower proton energies.

3. Analysis

3.1. TWO PARTICLE PICK-UP FORMALISM

The formula for the differential cross section for the two particle (p, τ) pick-up reaction, $\{\tau \equiv ^3\text{He}\}$ has been given by Glendenning ⁴⁾

$$\frac{d\sigma}{d\Omega} = \frac{k_\tau}{k_p} \frac{2J_\tau + 1}{2J_p + 1} \frac{m_\tau^* m_p^*}{(2\pi\hbar^2)^2} \sum_{LSJT} C_{ST}^2 \sum_{M_L} \left| \sum_N G_{NLSJT} B_{NL}^{M_L} \right|^2.$$

In this expression, N is the principal quantum number; L , S and J are the orbital, spin, and total angular momentum; T is the isospin, of the picked-up pair whilst in the target nucleus;

$$C_{ST}^2 = |(T_i T_{zf}, T T_z | T_i T_{zi})|^2 \frac{1}{2} (\delta_{S0} \delta_{T1} + \delta_{S1} \delta_{T0}),$$

where the suffices i and f refer to the initial and final nuclei;

$$B_{NL}^{M_L} = (-1)^{L+M_L} i^{-L} (2L+1)^{-\frac{1}{2}} \int \{ \psi_p^{(-)}(-\mathbf{k}_p, \mathbf{R}_p) u_{NL}(R) Y_L^{-M_L}(\hat{\mathbf{R}}) \}^* V(\rho) \times \psi_\tau^{(+)}(-\mathbf{k}_\tau, \mathbf{R}_\tau) \phi(\rho) d\mathbf{R}_p d\mathbf{R}_\tau,$$

in which the R are the centre of mass co-ordinates of the incident and outgoing particles and of the picked-up pair whilst in the ^6Li nucleus; $\phi(\rho)$ describes the relative motion, in the ^3He , of the proton and the centre of mass of the picked up pair; ψ_p and ψ_τ describe the entrance and exit channel elastic scattering; $u_{NL}(R)$ is the radial wave function of the centre of mass of the picked up pair whilst in the target nucleus; $V(\rho)$ is the interaction between the proton and the centre of mass of the picked-up pair:

$$G_{NLSJT} = \sum_{\substack{n_1 l_1 \\ n_2 l_2}} \beta_{n_1 l_1 n_2 l_2; LSJT} \Omega_n \langle n0, NL; L | n_1 l_1, n_2 l_2; L \rangle,$$

where

$$\beta_{n_1 l_1 n_2 l_2; LSJT}(\mathbf{J}_f, \mathbf{J}_i) = \binom{A+2}{A}^{\frac{1}{2}} \int [\psi_{J_f T_f}^*(A) \phi_{\gamma LSJT}(\mathbf{r}_1, \mathbf{r}_2)]_{J_i T_i} \times \psi_{J_i T_i}(A, \mathbf{r}_1, \mathbf{r}_2) dA d\mathbf{r}_1 d\mathbf{r}_2$$

is the parentage factor connecting the nucleus $(A+2)$ to (A) , \mathbf{r}_1 and \mathbf{r}_2 being the co-ordinates of the individual particles of the picked-up pair whilst in the target nucleus, and the square brackets denote vector coupling;

$$\Omega_n = \int u_{n\lambda}(r) u_{n,l}(r) r^2 dr$$

is the overlap of the relative motion of the picked-up pair in the target nucleus and in the ${}^3\text{He}$; and the bracket $\langle n\lambda, NA; L|n_1 l_1, n_2 l_2; L \rangle$ transforms the wave function of the picked-up pair, whilst in the target nucleus, from individual co-ordinates \mathbf{r}_1 and \mathbf{r}_2 , to centre of mass and relative co-ordinates \mathbf{R} and \mathbf{r} , according to the relation

$$[\phi_{n_1 l_1}(\mathbf{r}_1) \phi_{n_2 l_2}(\mathbf{r}_2)]_L = \sum_{n\lambda NA} \langle n\lambda, NA; L|n_1 l_1, n_2 l_2; L \rangle [\phi_{NA}(\mathbf{R}) \phi_{n\lambda}(\mathbf{r})]_L,$$

where once again the square brackets denote vector coupling. Here, λ must be zero, and therefore $A = L$, for non zero overlap with the assumed pure s-wave ${}^3\text{He}$ wave function in Ω_n .

The separation of the ${}^3\text{He}$ internal wave function into a factor $\phi(\rho)$ in the kinematic factor B_{NL}^{ML} and $u_{n,l}(r)$ in the structure factor, G_{NLSJT} , is made possible by assuming the wave function to be Gaussian.

Provided $\phi_{n_1 l_1}(\mathbf{r}_1)$, $\phi_{n_2 l_2}(\mathbf{r}_2)$, $\phi_{NA}(\mathbf{R})$, and $\phi_{n\lambda}(\mathbf{r})$ are taken to be harmonic oscillator wave functions, the transformation brackets can be obtained in closed form, and have been tabulated by Brody and Moshinsky⁵⁾.

3.2. EVALUATION OF THE STRUCTURE FACTOR

Using a Gaussian wave function for the ${}^3\text{He}$ internal motion, and assuming the particles in the ${}^6\text{Li}$ occupy the lowest oscillator states, the overlap integral Ω_n is given from Glendenning's expression⁴⁾ as

$$\Omega_0 = \left[\frac{2v\eta}{6\eta^2 + v} \left(\frac{6}{v} \right)^{\frac{1}{2}} \right]^{\frac{3}{2}},$$

where the ${}^3\text{He}$ size parameter $\eta = 0.206 \text{ fm}^{-1}$ and the ${}^6\text{Li}$ oscillator parameter $v = 11/6\langle r^2 \rangle$ [ref. 6)], where $\langle r^2 \rangle$ is the ${}^6\text{Li}$ mean square radius. The value of Ω_0 is very insensitive to $\langle r^2 \rangle$ being essentially unity for $\langle r^2 \rangle^{\frac{1}{2}}$ in the range 2.5 to 2.9 fm and falling to 0.96 for $\langle r^2 \rangle^{\frac{1}{2}} = 2.1$ or 3.4 fm. The value adopted for Ω_0 was 0.98 ± 0.02 .

A shell model calculation of the ground state of ${}^6\text{Li}$, by Barker⁷⁾ gives the components $0.992[2]^{13}\text{S}$, $-0.028[2]^{13}\text{D}$, and $0.120[11]^{11}\text{P}$ each of which represents an L - S coupled state, the notation being $[]^{2T+12S+1}L$ with $[]$ denoting the space symmetry of the wave function, $[2]$ for symmetric and $[11]$ for antisymmetric. In the

case of ${}^6\text{Li}$, the parentage factors reduce to the mixture co-efficients. Since the ${}^3\text{He}$ wave function is space symmetric, only the space symmetric components of the ${}^6\text{Li}$ wave function can contribute to the pick-up reaction, and since the $[2]^{13}\text{S}$ term is so very much stronger than the $[2]^{13}\text{D}$ term, only the $[2]^{13}\text{S}$ was considered in the pick-up analysis.

The quantum numbers in the transformation bracket $\langle n\lambda, N\Lambda; L|n_1 l_1, n_2 l_2; L\rangle$ are limited by

$$2(n+N)+\lambda+\Lambda = 2(n_1+n_2)+l_1+l_2,$$

and since $n_1 = n_2 = 0$, $l_1 = l_2 = 1$, and $n = 0$ for the ${}^6\text{Li}$ ground state, only one transformation bracket remains, namely $\langle 00, 10; 0|01, 01; 0\rangle$, which has the value $\sqrt{\frac{1}{2}}$ [ref. 5)].

The expression for G_{NLSJT} then reduces to the single term $G_{10110} = \beta_{0101;0110}\Omega_0 \langle 00, 10; 0|01, 01; 0\rangle = 0.687$, the isotopic spin factor C_{sT}^2 has the single value $C_{10}^2 = \frac{1}{2}$, and the differential cross section is given by

$$\frac{d\sigma}{d\Omega} = \frac{k_\tau}{k_p} \frac{2J_\tau+1}{2J_p+1} \frac{m_\tau^* m_p^*}{(2\pi\hbar^2)^2} \frac{1}{2} |G_{10110} B_{10}^0|^2.$$

3.3. EVALUATION OF THE KINEMATIC FACTOR

The only kinematic factor to be evaluated is

$$B_{10}^0 = \int \{\psi_p^{(-)}(-\mathbf{k}_p, \mathbf{R}_p) u_{10}(R) Y_0^0(\hat{\mathbf{R}})\}^* V(\rho) \psi_\tau^{(+)}(-\mathbf{k}_\tau, \mathbf{R}_\tau) \phi(\rho) d\mathbf{R}_p d\mathbf{R}_\tau.$$

This amplitude was found by using the DRC programme of Gibbs *et al.* ⁸⁾ to calculate the equivalent stripping amplitude

$$\int \{\psi_p^{(+)}(\mathbf{k}_p, \mathbf{R}_p) u_{10}(R) Y_0^0(\hat{\mathbf{R}})\}^* V(\rho) \psi_\tau^{(-)}(\mathbf{k}_\tau, \mathbf{R}_\tau) \phi(\rho) d\mathbf{R}_p d\mathbf{R}_\tau.$$

This calculation uses optical model wave functions in the elastic scattering channels, a Woods-Saxon potential for $u_{10}(R)$, and a zero range force for $V(\rho)$. The real wells in the elastic scattering channels were taken as standard Woods-Saxon type with radius, depth, and diffuseness given by R_1 , U_0 , and a_1 : the imaginary wells were surface type Woods-Saxon with parameters R_2 , W_0 , and a_2 . The radius of the charge distribution in the nucleus was taken equal to R_1 . No spin-orbit forces were included.

TABLE 1
Optical parameters for the elastic scattering channels

	${}^6\text{Li} + \text{p}$	${}^4\text{He} + {}^3\text{He}$
U_0 (MeV)	-59.5	-45
a_1	0.6	0.2
R_1 (fm)	2.27	3.4
W_0	0	0

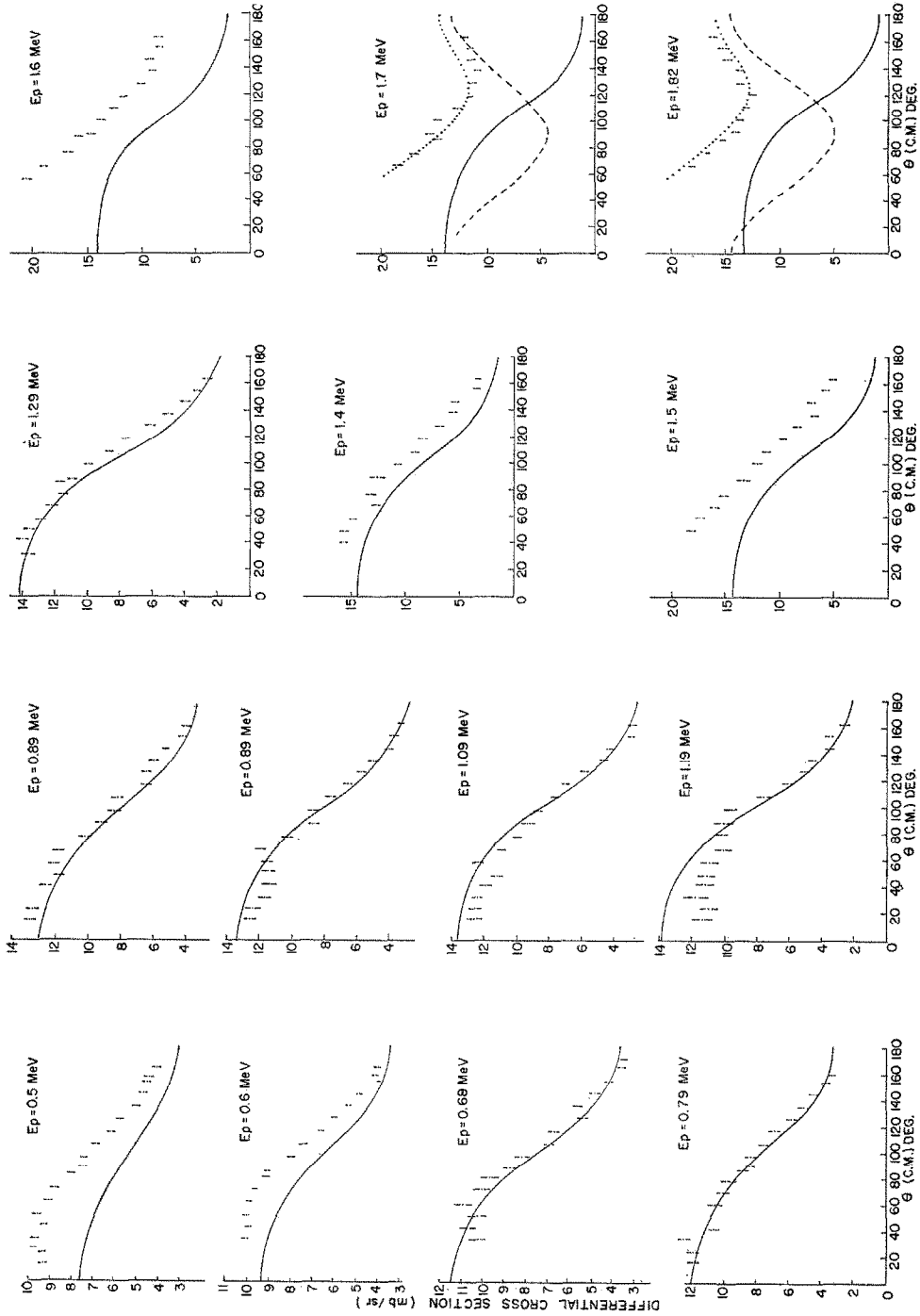


Fig. 3. Angular distributions of ${}^3\text{He}$ in the reaction $\text{Li}(p, {}^3\text{He}){}^4\text{He}$. The solid curves are the result of the two particle pick-up calculation, multiplied by the normalisation factor of 0.3. The broken curves are the results of resonant yield calculations, and the dotted line is an incoherent sum of the resonant and pick-up yields.

The proton optical parameters were obtained by fitting the ${}^6\text{Li} + \text{p}$ elastic scattering data of McCray ⁹⁾ at 0.495 MeV. The scattering is effectively pure Coulomb below 0.6 MeV, and the trivial fit corresponding to zero optical potential was rejected. The optimum parameter set had a near zero imaginary potential ($W_0 = -0.3$ MeV), consistent with the very small reaction cross section at this low energy. Putting $W_0 = 0$ had negligible effect on the results of the pick-up calculation, and this was done in the finally adopted set, given in table 1.

The ${}^3\text{He}$ optical parameters were obtained by fitting the elastic scattering data of Barnard *et al.* ¹⁰⁾ at 2.467 MeV and of Spiger and Tombrello ¹¹⁾ at 7.199 MeV. The s-, p-, and d-wave phase shifts were calculated as a function of real well depth, and compared with the experimental values of Spiger and Tombrello. Only two well depths correctly reproduced all three experimental phase shifts, and this served to pick out two parameter sets from those which gave good fits to the angular distributions. Both parameter sets were tried in the pick-up calculation; one set gave pick-up angular distributions peaked near 90° in clear disagreement with experiment, and was rejected; the other set gave forward peaked angular distributions and was adopted. It is given in table 1.

4. Results

The angular distributions are shown in fig. 3. The experimental data have been normalised to the absolute values of Marion *et al.* ¹⁾ at 0.8 MeV, corrected with the normalisation factor of Harrison ¹²⁾. The solid curves are the results of the pick-up calculation, multiplied by an arbitrary normalisation factor of 0.3. Above 1.3 MeV, the effects of the 1.82 MeV resonance start to be felt, and the direct reaction calculation curve falls below the experimental data. At 1.7 and 1.82 MeV, the resonant cross section was calculated using the resonance parameters of McCray ⁹⁾ and the normalisation of Harrison ¹²⁾; this is shown as the broken line in fig. 3. The dotted line in the figure is the simple sum of the direct and resonant cross sections, with no interference terms considered.

5. Discussion

The direct reaction calculation is remarkably successful in reproducing the shape of the angular distributions at energies sufficiently far removed from the resonance, i.e. below 1.3 MeV. Since the same normalisation factor is used throughout, it is clear that the calculation also reproduces well the energy dependence of the cross section in this energy range. Further, the results at 1.7 and 1.82 MeV are strongly suggestive that the pick-up calculation successfully gives the non-resonant cross section right up to the resonance energy itself.

The need for the arbitrary normalisation factor of 0.3 is unfortunate, but perhaps not surprising, in view of the approximations involved in the calculation.

The Gaussian wave function for ${}^3\text{He}$, and the zero range force for the interaction between the incident proton and the picked-up pair are chosen on algebraic, not physical, grounds. In addition, we have been somewhat cavalier in assuming $u_{n0}(r)$ and $u_{NL}(R)$ were harmonic oscillator waves functions where this had algebraic advantages (in evaluating the overlap integrals $\langle n0, NL; L | n_1 l_1, n_2 l_2; L \rangle$ and Ω_n) and then using the more realistic Woods-Saxon wave function for $u_{NL}(R)$ in the calculation of B_{NL}^{ML} which determines the shape of the angular distributions.

The use of such approximations can possibly be justified for this particular reaction on the grounds that the calculation could be reduced to a single term, and it is to be expected that the use of more realistic wave functions for the ${}^3\text{He}$ and $u_{n0}(r)$ and $u_{NL}(R)$ throughout would affect the normalisation, through the overlap integrals, but have little effect on the shape. The zero range approximation is also expected to affect the normalisation rather than the shape. We therefore consider the success of direct pick-up theory in accounting for the non resonant yield over the whole energy range, with a modest constant normalisation factor to be impressive, and to show that the angular distributions can be accounted for without recourse to postulating the existence of low lying positive parity levels in ${}^7\text{Be}$.

It is a pleasure to acknowledge very helpful discussions with Prof. T. A. Tombrello concerning the use of the ${}^3\text{He}$ - ${}^4\text{He}$ elastic scattering data, and also to extend thanks to Dr. J. R. Bird for the hospitality of the Australian Atomic Energy Commission Laboratory, and to the many members of his staff who helped in the running of the experiment.

References

- 1) J. B. Marion, G. Weber and F. S. Mozer, *Phys. Rev.* **104** (1956) 1402
- 2) H. Beaumevielle, J. P. Longequeue, N. Longequeue and R. Bouchez, *J. de Phys.* **25** (1964) 933
- 3) S. Bashkin and G. Goldhaber, *Rev. Sci. Instr.* **22** (1951) 122
- 4) N. L. Glendenning, *Phys. Rev.* **137** (1965) B102
- 5) T. A. Brody and M. Moshinsky, *Tables of transformation brackets* (Monografias del Instituto de Fisica, Mexico, 1960)
- 6) M. A. Moszkowski, *Handbuch der Physik*, ed. S. Flügge, vol. 39 (Springer Verlag, Berlin, 1957) p. 468
- 7) F. C. Barker, *Nucl. Phys.* **83** (1966) 418
- 8) W. R. Gibbs, V. A. Madsen, J. A. Miller, W. Tobocman and E. C. Cox, *National Aeronautics and Space Administration report NASA TN, D-2170* (1964)
- 9) J. A. McCray, *Phys. Rev.* **130** (1963) 2034
- 10) A. C. L. Barnard, C. M. Jones and G. C. Phillips, *Nucl. Phys.* **50** (1964) 629
- 11) R. J. Spiger and T. A. Tombrello, *Phys. Rev.* **163** (1967) 964
- 12) W. D. Harrison, *Nucl. Phys.* **92** (1967) 261